

Lithospheric-scale seismic interferometry: a comparison of approaches to deal with an irregular source distribution and source-side reverberations

Elmer Ruigrok¹, Xander Campman² and Kees Wapenaar¹

¹ Delft University of Technology, Department of Geotechnolgy

² Shell International Exploration & Production B.V.

I. INTRODUCTION

A variety of seismic methods has been developed to image the lithosphere using the responses from distant earthquakes. On the one hand, there are the tomographic methods, that use either surface waves or body waves to obtain a low-resolution velocity-variation distributions. On the other hand, there are methods that use body waves to obtain a reflectivity image. In the later class, especially Receiver Function (RF) methods (Wilson & Aster, 2005), which image converted waves, are popular. RF are successful in obtaining an estimate of the large impedance contrasts, though the resolution is limited due to a few practical limitations.

An attractive alternative for RF would be to apply seismic interferometry (SI). Green's function retrieval or SI refers to the principle of generating new seismic responses by crosscorrelating seismic observations at different receiver locations. This technique is frequently used for the retrieval of surface waves between seismic stations since pioneering work by Campillo & Paul (2003), but can in principle be used to retrieve a complete Green's function (Wapenaar, 2004), dependent on the distribution of actual sources. When a collection of reflection responses is obtained using SI, one for a virtual source at each station position, a high-resolution reflectivity image can be obtained by using standard exploration-scale processing (Yilmaz *et al.*, 2000) as is shown by Draganov *et al.* (2009) for an exploration-scale passive dataset. A similar processing sequence could be used for lithospheric imaging. The advantages with respect to RF imaging would be 1) that SI can be applied on the Z-component only (decomposition can be left out), 2) the source-time-function deconvolution may be omitted, 3) free-surface-reflected phases are automatically used, without any model information required and 4) multiple information is suppressed in the stacking process.

It was previously realized by a number of researchers (Abe *et al.*, 2007; Fan *et al.*, 2006; Kumar & Bostock, 2006; Schuster *et al.*, 2004) that SI may well be applied to transmission responses from distant earthquakes, detected by broadband seismic stations. Two relevant issues were previously unaddressed, 1) irregular source distribution and 2) source-side reverberations.

In this study, we test which SI approach can be used best to deal with an irregular illumination and -at the same time- adequately suppresses artifacts caused by source-side reverberations. For these tests we generate

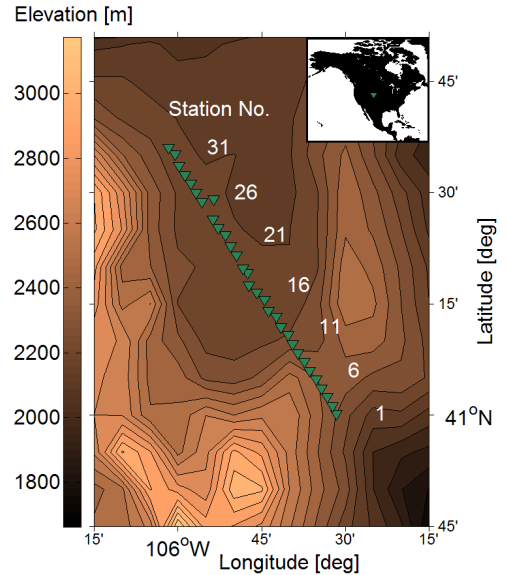


FIG. 1 The Laramie array of broadband stations (green triangles) and the local topology (colormap). The inset in the upper right-hand corner depicts North America and the array location.

synthetic data with similar source-side reverberation, and illumination, characteristics as an actual dataset from the Laramie broadband array (2000-2001).

II. MODELING

Fig. 1 shows the layout of the Laramie array. Only P-wave data is forward modeled. Thus, the assumption is made, that the actual data would be decomposed, or that the Z-component would be a good estimate of the P-wave component. For the modeling, the stations sampling is regularized. On Fig. 2, a simplified crustal model for the subsurface under this array, is depicted. The mean feature is a Moho at 40 km depth. This model is used for forward modeling transmission responses in a frequency band of 0.5-1.5 Hz.

In Wapenaar & Fokkema (2006) a SI relation is derived for a configuration with illumination from below and receivers on a free surface. This SI relation consists of a surface integration of correlations over source positions. For a regional array of receivers, an incoming wave caused by a distant earthquake is by approximation a plane wave.

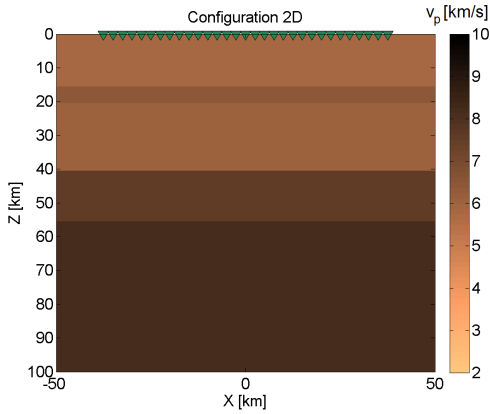


FIG. 2 A simplified horizontally layered velocity model for the crust and upper mantle below the Eastern Rocky Mountains. The model was derived from a refraction survey (Chulick & Mooney, 2002)

Consequently, each global phase, e.g., P, PP, PcP and PKP, may be treated as a separate effective plane-wave source, characterized by a single rayparameter \mathbf{p} . For earthquakes that are more or less inline with a receiver array, different phases may be characterized with a single horizontal rayparameter p . Thus, we rewrite the relation from Wapenaar & Fokkema (2006) to an integration over p :

$$\int_{\partial\mathcal{S}_1} G(\mathbf{x}_A, p, -t) * G(\mathbf{x}_B, p, t) dp \approx G(\mathbf{x}_A, \mathbf{x}_B, -t) + G(\mathbf{x}_A, \mathbf{x}_B, t), \quad (1)$$

where $G(\mathbf{x}_A, p, t)$ denotes the Green's function observed at \mathbf{x}_A (one of the stations) due to a plane wave source with rayparameter p . \mathcal{S} is a vertical section through the receivers and the medium of interest and $\partial\mathcal{S}_1$ is the lower part of the enclosing line in the lower half space, see Fig. 3(a). The retrieved response $G(\mathbf{x}_A, \mathbf{x}_B, t)$, would be the Green's function between two receiver positions, \mathbf{x}_A and \mathbf{x}_B . To retrieve a response between one station \mathbf{x}_A and all the other stations, equation 1 would need to be repeated for varying \mathbf{x}_B (Fig. 3(b)). Effective sources on $\partial\mathcal{S}_1$ correspond to small rayparameters. These rayparameters contribute to the retrieval of body waves at near and intermediate offsets.

With equation 1 both a causal and a anticausal response is retrieved. This is explained in Fig. 4. A reflection between \mathbf{x}_A and \mathbf{x}_B can be retrieved at positive times by contributions from sources with negative p . The same reflection can be retrieved at negative times by contributions from sources with positive p . The standard procedure would be to add the time-reversed anticausal result of equation 1 to the causal result, to increase the signal-to-noise ratio. Alternatively, the contributions from the positive rayparameters can be time-reversed prior to integration. Hence, only a response is retrieved at positive times, but the sampling of the integral is increased by a factor of 2. Thus, especially when the sampling of

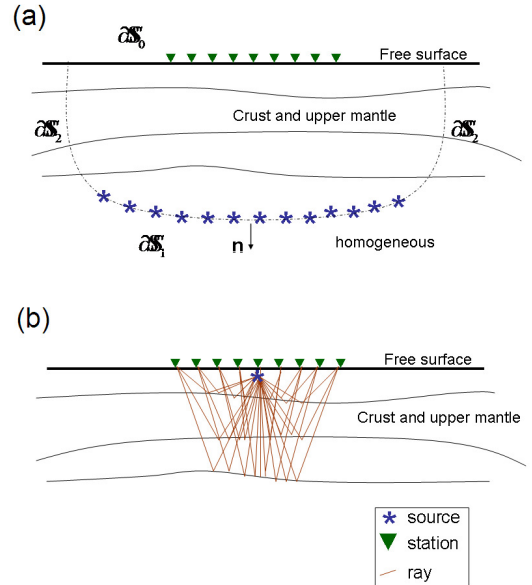


FIG. 3 (a) the configuration for regional-scale seismic interferometry, an approximately layered medium with illumination from below and a recording of responses on the free surface. (b) the retrieved response between the middle station and all the other stations. Note that only the retrieved primaries are depicted with rays, whereas in reality also free-surface and internal multiples would be retrieved.

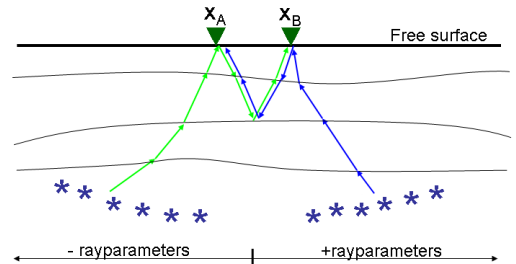


FIG. 4 The two specular rays for retrieving a reflection between a station at \mathbf{x}_A and at \mathbf{x}_B .

equation 1 is just insufficient, it is advantageous to apply time-reversal prior to integration. In the following we will call this the TRBI approach.

The moment tensor of an earthquake is of little relevance for this application of SI, since it may be assumed that the array lays within one focal plane. In this case, the observed response at \mathbf{x}_A may be written as a convolution of a source-time function (STF) with the Green's function $G(\mathbf{x}_A, p, t)$. By assigning a STF to the observed Green's functions in equation 1, the retrieved response will be a convolution of the Green's function between \mathbf{x}_A and \mathbf{x}_B with a stack of autocorrelations of all individual STF's. Through the autocorrelation, the STF's become all zero-phase, which facilitates a successful stacking (integration), even when earthquake responses have very

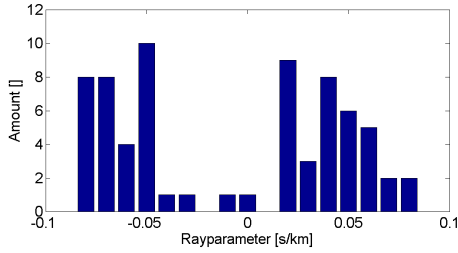


FIG. 5 A histogram distribution of the different phase-responses. Each phase response is represented by one rayparameter. In total there are 69 phase responses. The binsize is 0.01 s/km.

different -and very complicated- STF's.

A. Irregular source distribution

During the array's deployment, which was about half a year, numerous high-quality earthquake responses were recorded. As a first selection criteria we take responses caused by earthquakes with a magnitude larger than 5. We further restrict the pool by taking only responses caused by earthquakes from within the 1st Fresnel zone for direct waves and with acceptable data quality. We end up with 39 earthquake responses, from which we can extract 69 separate phase responses. The p distribution of these effective sources is depicted in Fig. 5).

In Fig. 6 different approaches are tested to deal with an irregular source sampling. In (a) the reference response is shown. This is a synthesized response for a source at $x=40$ km (stations 16). A primary reflection from all 4 interfaces can be distinguished. In addition, a 1^{st} order multiple from the upper three interfaces can be seen. (c)-(e) are retrieved responses with equation 1 after adding the time-reversed anticausal result to the causal part and muting early times.

Comparing the retrieved responses (b)-(f) with the reference response (a), it can be seen that the first two reflections are not retrieved correctly for any SI approach. Due to the limited illumination, reflections from the shallow interfaces are not retrieved correctly (that is, with a smaller slope than the actual reflections) at large offsets. For this reason, early times at larger offsets are normally muted. In (b), nothing is done to take the source irregularity into account. Large artifacts can be seen, both due to overillumination and underillumination. Overillumination leads here to artifacts at times before an actual reflection and with a slope opposite to the actual reflection. Underillumination leads here to the retrieval of the near-offset with smaller frequencies than the actual ones. If the irregular spacings are approximately known, the rayparameter domain can be divided into bins and the

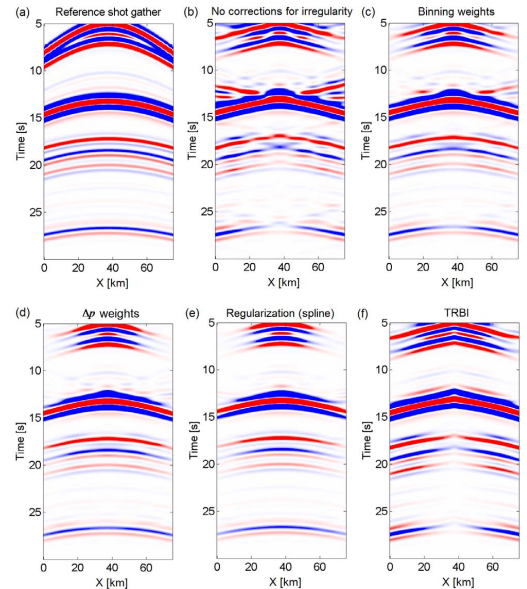


FIG. 6 Responses estimated with SI, with different adjustments for source irregularity, compared with the reference response (a). In (b) no adjustment is applied, in (c) binning weights are applied, in (d) Δp is taken as a weight, in (e) the integrand is regularized using spline interpolation and in (f) the TRBI approach is used.

traces can be weighted according to the amount of traces per bin (c). As a binsize 1 s/km is taken (see Fig. 5). If the source locations are well known, every trace can be weighted by the distance to the neighboring traces (Δp) (d). Alternatively, the integrand may be regularized to a source spacing satisfying the sampling criterion for SI (e). The last 3 approaches (c), (d) and (e), are successful in suppressing overillumination artifacts. The artifacts due to underillumination are limited. For this synthetic data with perfectly coherent events, the integrand regularization (e) gives the best results. When the TRBI approach is used (f) the irregularity artifacts, also the ones due to underillumination, are suppressed. A disadvantage of this approach is that the near offset is not reconstructed well, since the stationary-phase regions (Snieder, 2004) for events in the near offset are only partly sampled.

B. Source-side reverberations

As an input for SI, transmission responses caused by distant earthquakes are used. With SI we aim to use the receiver-side reverberations. Though, the transmission responses also contain source-side reverberations. The different source-side reverberations may be described as separate effective sources. E.g., a direct P-phase is followed for most earthquakes by a pP and sP phase. The time difference between P, pP and sP is often not enough to untangle the receiver-side reverberations of these different phases. Therefore, SI is to be applied on a blend of effective sources. Nevertheless, the application of SI

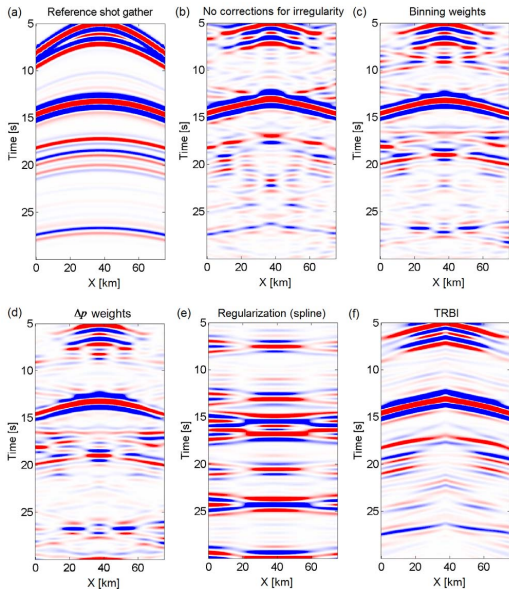


FIG. 7 Responses estimated with SI, with different adjustments for source irregularity, compared with the reference response (a). The used transmission responses contain 2 source-side reverberations. In (b) no adjustment is applied, in (c) binning weights are applied, in (d) Δp is taken as a weight, in (e) the integrand is regularized using spline interpolation and in (f) the TRBI approach is used.

needs to be such, that the spurious contributions caused by source-side reverberations are adequately suppressed.

A new synthetic dataset is created which does not only contain an irregular distribution of effective sources (Fig. 5), but which also contains source-side reverberations. In Fig. 7 again the same approaches are tested as in Fig. 6, but now the 'blended' transmission responses are used. For all approaches, a clear degradation of the quality of the retrieved responses can be noted, due to the additional crossterms. This degradation is worst for the regularization (e). The crossterms are different for each source, thus for each trace in a correlation panel (the integrand of equation 1). A straightforward spline interpolator cannot handle the large variations from trace to trace. This result might be significantly improved by a regularization algorithm with which random variation between traces are suppressed, see, e.g., Zwartjes & Sacchi (2007). The result of binning (c) and Δp (d) are quite bad, since different weights are given to the different cross terms in the correlation panel and therefore these crossterms stack out less successfully than when no weights are applied (b). The leftovers of the cross terms can be noted here as cross-shaped artifacts. The TRBI approach (f) gives the best results. Since no weights are applied, the cross terms stack out similarly as for (b), but additionally the source-sampling-irregularity artifacts are suppressed. Again the near offset is retrieved less successfully here, because of an amplitude reduction inherent to this SI strategy.

The blended transmission responses are used to re-

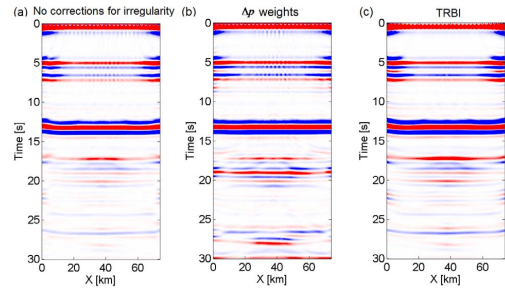


FIG. 8 Zero-offset stacks obtained from data retrieved with SI, using different adjustments for source irregularity. In (a) no adjustment is applied, in (b) Δp is taken as a weight, and for (c) contributions from sources with positive p are time-reversed prior to integration.

trieve 31 shotgathers, for a virtual source at each station position. Subsequently, the retrieved shot gathers are resorted to CMP (Common-Mid-Point) gathers. All CMP gathers are NMO (Normal Move-Out) corrected with the actual velocity model (Fig. 2 and stacked to obtain one zero-offset stack. This is the response as if there was a plane wave source at the free surface. The zero-offset stacks for the different methods are shown in Fig. 8. The resulting stacks for binning and regularization are left out.

Fig. 8(a) is a good estimate of the reflectivity of the subsurface. Only near zero time a spurious event can be seen, which is caused by using only a limited illumination range. The same spurious event can be noted in (b) and (c). The irregularity and source-blending artifacts, which were obvious on individual shotgathers (e.g., on Fig. 7(b)) have been suppressed. Contributions from multiples were partly suppressed in the stacking process. Fig. 8(b) shows the stack made with body-wave responses that were obtained with a Δp weighing SI approach. In this stack, artifacts caused by source-blending, remain. The stack that is made with body-wave responses from the TRBI approach (c) is similar to (a), though with a closer look it can be seen that the interfaces in (c) are more smooth than in (a).

Subsequently, the zero-offset stacks are migrated and converted from time do depth. The resulting images are depicted in Fig. 9. Since plane reflectors were imaged, the migration outcomes are similar to the zero-offset stacks.

III. CONCLUSIONS

We studied retrieving body-wave responses between a regional array of broadband stations using SI. SI consists of a surface integration of correlations over source positions. It is important to obtain enough effective sources from actual earthquakes to adequately sample this integral. We showed, with numerical data, that a few months of data suffices to select a good distribution of

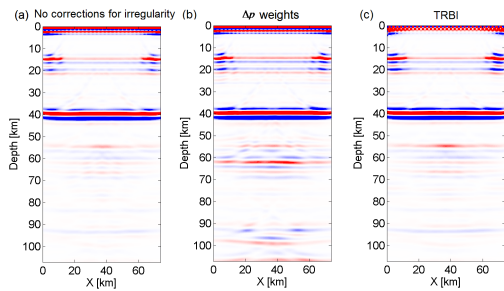


FIG. 9 Post-stack migrated and time-to-depth converted images, obtained from data retrieved with SI, using different adjustments for source irregularity. In (a) no adjustment is applied, in (b) Δp is taken as a weight, and for (c) contributions from sources with positive p are time-reversed prior to integration.

sources, at least, when the array is more or less inline with an earthquake belt. The irregularity of this distribution introduces over- and underillumination artifacts to the retrieved responses. These artifacts can be suppressed by weighing the contributions to the integrand with the distances between the effective sources, or by regularizing the integral. When, in addition, the influence of source-side reverberations is taken into account, a weighing strategy degrades the result. In this case, the best reflection response can be obtained when contributions from effective sources with positive rayparameters are time-reversed prior to integration (TRBI approach). We further processed the retrieved body-wave responses to reflectivity images. It turns out that, in this process, irregularity and source-blending artifacts are sufficiently suppressed. Only when a weighing strategy was used to obtain the body-wave reflections, source-blending artifacts remain. In conclusion, we can state that a straightforward implementation of SI suffices if the eventual goal is to obtain a reflectivity image. If also the retrieved body-wave responses are studied, it is better to use the TRBI approach.

Acknowledgments

This work is supported by The Netherlands Organization for Scientific Research (NWO).

References

- Abe, S., Kurashimo, E., Sato, H., Hirata, N., Iwasaki, T., & Kawanaka, T., 2007. Interferometric seismic imaging of crustal structure using scattered teleseismic waves, *Geophysical Research Letters*, **34**, L19305.
- Campillo, M. & Paul, A., 2003. Long-range correlations in the diffuse seismic coda, *Science*, **299**, 547–549.
- Chulick, G.S. & Mooney, W.D., 2002. Seismic structure of the crust and uppermost mantle of North America and adjacent oceanic basins: a synthesis, *Bulletin of the Seismological Society of America*, **92**, 2478–2492.
- Draganov, D., Campman, X., Thorbecke, J., Verdel, A., & Wapenaar, K., 2009. Reflection images from seismic noise, p. in press.
- Fan, C., Pavlis, G.L., Weglein, A.B., & Nita, B.G., 2006. Removing free-surface multiples from teleseismic transmission and constructed reflection responses using reciprocity and the inverse scattering series, *Geophysics*, **71**, SI71–SI78.
- Kumar, M.R. & Bostock, M.G., 2006. Transmission to reflection transformation of teleseismic wavefields, *Journal of Geophysical Research*, **111**, B08306.
- Schuster, G.T., Yu, J., Sheng, J., & Rickett, J., 2004. Interferometric/daylight seismic imaging, *Geophysical Journal International*, **157**, 838–852.
- Snieder, R., 2004. Extracting the Green's function from the correlation of coda waves: a derivation based on stationary phase, *Physical Review E*, **69**, 046610–1–046610–8.
- Wapenaar, K., 2004. Retrieving the electrodynamic green's function of an arbitrary inhomogeneous medium by cross-correlation, *Physical Review Letters*, **93**, 254301–1–254301–4.
- Wapenaar, K. & Fokkema, J.T., 2006. Green's functions representations for seismic interferometry, *Geophysics*, **71**, SI33–SI46.
- Wilson, D. & Aster, R., 2005. Seismic imaging of the crust and upper mantle using regularized joint receiver functions, frequency-wave number filtering, and multimode kirchhoff migration, *Journal of Geophysical Research*, **110**, B05305.
- Yilmaz, O., Doherty, S.M., & Yilmaz, O., 2000. *Seismic Data Analysis: Processing, Inversion and Interpretation of Seismic Data*, SEG.
- Zwartjes, P.M. & Sacchi, M.D., 2007. Fourier reconstruction of nonuniformly sampled, aliased seismic data, *Geophysics*, **72**, V21–V32.